Journal of Manufacturing Processes 73 (2022) 903–913

Contents lists available at ScienceDirect

Journal of Manufacturing Processes

journal homepage: www.elsevier.com/locate/manpro

# Study on material removal mechanisms in electrochemical etching-enhanced polishing of GaN

Linfeng Zhang, Dong Lu, Hui Deng *

*Department of Mechanical and Energy Engineering, Southern University of Science and Technology, No. 1088, Xueyuan Road, Shenzhen, Guangdong 518055, China*

A R T I C L E I N F O

*Keywords:*
Electrochemical etching
Polishing
Surface carrier accumulation
Ductility

A B S T R A C T

Electrochemical etching has been proven to be a highly effective method for the removal of GaN materials. In this work, the material removal mechanisms in electrochemical-enhanced polishing process are studied from two aspects: carrier behavior and mechanical removal. It is found that the distribution of carriers can be altered along the polar plane by the electric field during electrochemical etching and will not recover spontaneously. A layer of excess carriers would accumulate on the Ga-face after electrochemical etching and cause severe surface oxidation during sample preservation. Additionally, it is revealed that the etched surface morphology can be divided into two types: protrusions and pits, depending on the excessive carrier density. Mechanical polishing is conducted on the pre-etched and non-etched surface, respectively. The pre-etched surface demonstrates better ductility than that of the non-etched surface owing to the formation of porous structure during electrochemical etching. The surface quality is also desirable which is confirmed by the photoluminescence (PL) spectra. The electrochemical etching-enhanced polishing can be considered as a semi-final processing technique that efficiently removes the damaged layer and reduces the surface roughness to sub-nanometer level.

## 1. Introduction

GaN is a promising next-generation semiconductor material due to its excellent chemical and electrical properties, such as wide bandgap, high electron mobility, and breakdown voltage. These properties make GaN devices have a wide range of high-power and high-frequency applications, and the most representative device is the GaN-based High Electron Mobility Transistor (HEMT) [1,2]. In AlGaN/GaN HEMTs, the strong electronegativity difference between Ga and N atoms creates spontaneous polarization in the GaN crystal, resulting in high-density two-dimensional electron gas (2DEG), thereby reducing the on-resistance values [3,4].

The electronegativity difference also makes GaN has a larger proportion of ionic bonds, which leads to a more obvious brittleness of GaN [5,6]. Wafer processing was carried out before epitaxial growth to correct wafer thickness and reduce surface roughness. Wafer processing usually involves a series of material removal processes such as slicing, grinding, lapping, mechanical polishing, and finally chemical mechanical polishing (CMP) [7–10]. The high brittleness of GaN makes it easier to fracture into large pieces by abrasion rather than being plastically removed in the conventional mechanical polishing method using abrasives [8,11]. Therefore, some deep cracks and a thick subsurface damaged (SSD) layer are inevitably formed which would be entirely removed by CMP with a very long duration of more than 100 h [12].

Many efforts have been conducted to improve the efficiency of GaN wafer processing. Dry etching techniques such as inductively coupled plasma etching have a high etching rate and can efficiently remove the SSD layer induced by grinding or lapping [13]. However, dry etching is highly anisotropic, which means that it has less planarization effect. In addition, dry etching is prone to form ion-induced damage [14–16]. For semiconductor materials such as silicon, wet chemical etching combines surface oxidation and dissolution of oxide products and is considered to be a low-cost and damage-free etching technique [17]. However, GaN has excellent chemical stability due to the strong Ga—N bonding. It is hard for the c-plane of GaN to be etched using conventional acid or alkaline solvent at room temperature [18,19]. To date, the wet chemical etching of GaN using hot $H_3PO_4$, a mixture of $H_3PO_4$ and $H_2SO_4$, and molten KOH have been widely studied [20–22]. However, conventional chemical wet etching with conventional etchants of GaN always has a low etching rate of typically 50 nm/h due to its chemical inertness. Besides, etching will occur preferentially at defects, forming etching pits and reducing surface integrity [23–25].

---

* Corresponding author.
*E-mail address:* dengh@sustech.edu.cn (H. Deng).

https://doi.org/10.1016/j.jmapro.2021.11.059
Received 6 August 2021; Received in revised form 17 October 2021; Accepted 26 November 2021

Photoelectrochemical etching (PECE) and electrochemical etching (ECE) have been employed to enhance the etching process and achieve uniform material removal with the aid of an external electric field or ultraviolet (UV) illumination. A great deal of previous research into PECE has focused on defects investigation, damage removal, relationship of etching features and defects [26–30]. In the PECE process, GaN is irradiated by a UV source and electron-hole pairs, which reduce the interatomic strength and enhance the chemical reaction, are generated [31]. Dong et al. developed a novel method called photoelectrochemical mechanical polishing (PECMP). PECMP combined photoelectrochemical etching to efficiently remove the SSD layer and abrasive polishing to smooth the surface. The surface roughness Ra decreased from 1.04 nm to 0.067 nm in 135 min. The cathodoluminescence (CL) spectra also demonstrate that the PECMP method could remove the scratches and SSDs [32,33]. Electrochemical etching has been applied in the fabrication of porous structures for gas sensors and solar cells [34]. In the electrochemical etching, the electron-hole pairs are generated by the avalanche breakdown or electron tunneling under the action of the electric field [35]. The holes are injected into the GaN surface and form an oxide layer which is then dissolved in the electrolyte, while the excessive electrons are consumed at the cathode. In our previous study, it has been demonstrated that electrochemical etching can achieve a high material removal rate (MRR) of GaN and the etched surface can be efficiently smoothed by CMP process [36]. However, the material removal mechanisms in electrochemical etching and abrasive polishing are still not clear. Clarification of these mechanisms is beneficial to understand the electrochemical etching-enhanced polishing process and better apply this technique effectively on GaN wafer processing.

This research provides some important insights into the mechanisms of material removal in the electrochemical etching-enhanced polishing process of GaN. The phenomenon of excessive carrier accumulation on the Ga-face after electrochemical etching is studied. And the correlation between the surface carrier density and the etched surface morphology is investigated. Eventually, the mechanical properties of the etched and non-etched GaN surfaces are compared.

## 2. Experimental details

Commercially available Si-doped n-type freestanding GaN wafers supplied by Suzhou Nanowin Co. Ltd. were used in this study. The size of the GaN wafer is $10 \times 10.5$ mm$^2$ with a thickness of $350 \pm 25$ μm. The dislocation density of the wafer is about $5 \times 10^6$ cm$^{-2}$. The electrical conductivity is slightly lower than 0.05 Ω·cm.

Before the electrochemical etching process, each sample was immersed in absolute ethyl alcohol for 5 min to remove the surface contamination. Then, the wafer was flushed by deionized water for 30 s and dried off by a nitrogen gun. In the electrochemical etching process, NaOH solution was selected as the electrolyte based on the results of the previous study. The GaN substrate was used as the working electrode while a platinum mesh ($2 \times 2$ cm$^2$) was set as the counter electrode. The Ga-face (c+ plane) was in contact with the electrolyte while the N-face (c− plane) was linked to the anode. A resin mask with a circular hole in the center was placed between the sample and the electrolyte. The hole was 8 mm in diameter and was set to be concentric with the sample. Hence, only a circular region located in the center of the sample was in contact with the NaOH solution. The etching only occurred in this circular region and other surface area is covered. After electrochemical etching, each sample was flushed by deionized water for 30 s to wash down the residual electrolyte and dried off. A DC power (Keithley 2280s-60-3) supplied the constant voltage for electrochemical etching. All chemical reagents were provided by EMD Millipore Co., Ltd.

The surface morphology was measured by scanning electron microscopy (SEM, Zeiss Merlin). The surface morphology and Sa surface roughness were measured using atomic force microscopy (AFM, Bruker Dimension Edge), operating in tapping mode with a silicon tip. The chemical composition of GaN surface with or without carrier accumulation was evaluated by X-ray photoelectron microscopy (XPS, Quantum 2000, ULVAC-PHI) with AlKα radiation (1486.6 eV). The X- ray source was operated at 50 W with a constant pass energy of 69 eV for all samples. The surface quality was studied by photoluminescence (PL) with a helium-cadmium (He—Cd) laser excitation source emitting at 325 nm. The nano-indentation tests were performed by a nanoindenter system (Hysitron Ti-950).

## 3. Results and discussion

### 3.1. Surface carrier accumulation

One finding of this study was that excessive carriers would be accumulated on the surface of GaN after electrochemical etching. As introduced previously, wurtzite GaN has excellent chemical stability due to the strong bonding of Ga—N. It has been proved that GaN cannot be etched at room temperature by many powerful solvents including NaOH solution [19]. In previous studies, it has been proved that the etching of GaN occurs under the combined action of excessive holes and hydroxyl ions. That is to say, once sufficient excessive carriers exist on the surface, the etching behaviors could be observed on the surface after rinsed in the NaOH solution. In this work, the existence of excessive carriers on the surface was examined by the NaOH solution.

To investigate the formation mechanism and distribution of the surface carrier accumulation, five identical as-received GaN samples numbered I to V were used in this experiment. Fig. 1 shows the experimental steps of verifying surface excessive carrier accumulation. In the initial stage, all samples were electrochemically etched in 5 wt% NaOH solution with a potential of 60 V for 20 min to form a sufficient number of carriers on the surface. After that, the samples were kept for over 24 h without any treatment. In the next step, three basic methods, labeled as method A, B, and C, were employed to process these five samples. For method A, a non-uniform inverse electric field was applied by point contact electrode. For method B, a uniform inverse electric field was applied by surface contact electrode. For method C, 9 h of CMP was carried out on the etched substrate to remove the outermost surface of material. Sample I was served as the control group without any further treatment. Sample II, III, IV were processed by method A, B, and C, respectively. Sample V was processed by method B and subsequently method C. Finally, all the samples were immersed in the NaOH solution with a weight concentration of 5 wt% for 20 min. The purpose of this step is to confirm whether there are carriers on the surface. The samples were then rinsed by deionized water and dried off for further surface observation. External electric field is supposed to be the main factor in the formation of surface carrier accumulation and its effect on the surface carrier accumulation also needs to be confirmed. Therefore, the sampling area is selected to be about 1 mm away from the circular pre-etched area, where only electric field acts on. In addition, the surface outside the pre-etched area is flat, and the changes in surface morphology can be observed more clearly.

The details about the treatment methods are listed as follows. When applying the inverse electric field, a pair of identical titanium plates was used as the electrode. The surfaces of titanium plates were polished to be relatively flat to have good contact with the sample. The Ga-face was linked to the anode, while the N-face was linked to the cathode. The resulting electric field was in the opposite direction to that of electrochemical etching, namely an inverse electric field is applied. For inverse electric field, the applied voltage was 30 V and the duration was 20 min. In the CMP process, the polishing pressure was 0.5 kg/cm$^2$ and the rotation speed of the spindle was 1000 rpm. $CeO_2$ slurry with an abrasive size of 0.75 μm was used in the CMP process.

As shown in Fig. 2(a), the surface of the as-received sample is very smooth and no obvious etching can be observed. It is shown that GaN cannot be directly etched by NaOH solution at room temperature. Fig. 2 (b) shows the surface morphology of sample I. After immersed in the

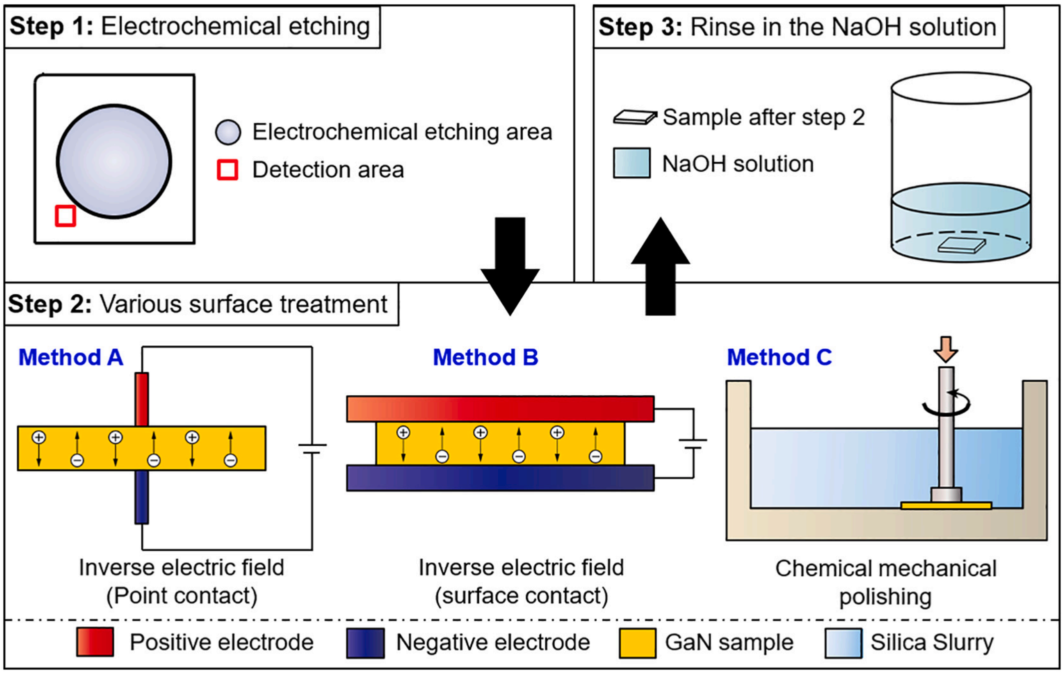

**Fig. 1.** Schematics of experimental steps in the verification of surface excessive carrier accumulation.

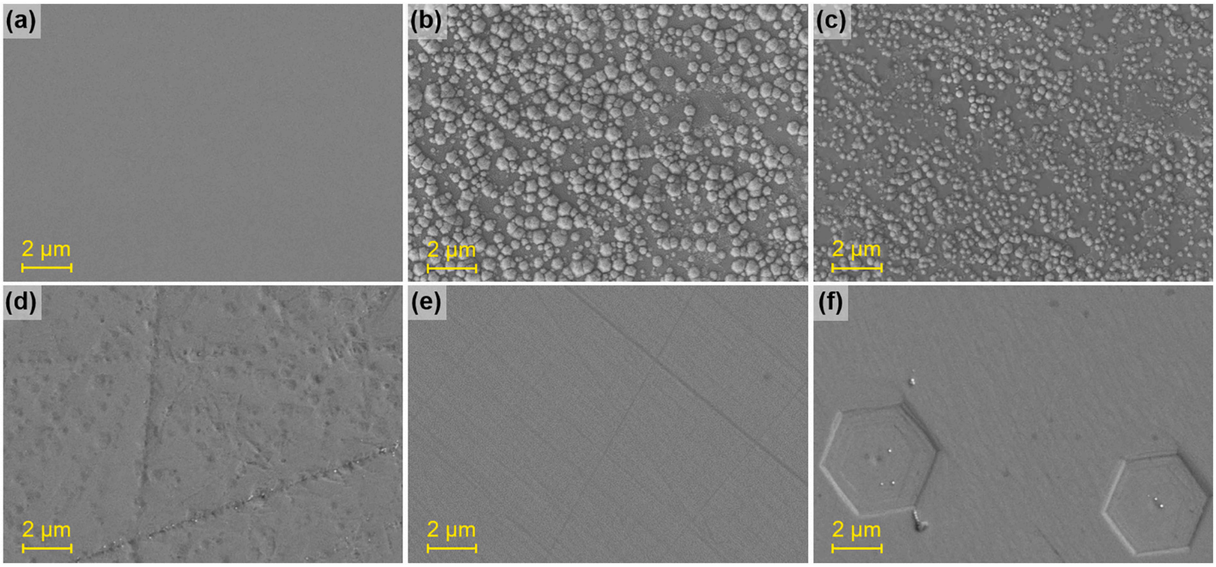

**Fig. 2.** GaN surface morphology after rinsed in the NaOH solution with different pre-treatment processes of (a) as-received sample and (b–e) sample I to V, respectively.

NaOH solution, protrusions which can be considered as the etching characteristics are generated on the Ga-face of the sampling region. These results show that electric field can change the distribution of carriers. However, no obvious etching characteristics can be observed on the N-face. The results indicate that there are sufficient excessive carriers on the Ga-face, while very few excessive carriers exist on the N-face. The etching characteristics of sample II become less obvious as shown in Fig. 2(c). It indicates that the excessive carrier density on the Ga-face declines under the action of inverse electric field. For sample III, only the scratches are etched, indicating a fairly low surface carrier density after applying a uniform inverse electric field as shown in Fig. 2 (d). It means that a uniform electric field can more efficiently redistribute the carriers from surface to substrate. As the surface carrier density decreases, the etching characteristics change from protrusions to pits, indicating the change of material removal mode. The change of material removal mechanisms will be discussed in detail in the following section. Fig. 2(e) shows the surface morphology of sample IV which was applied by an inverse electric field and subsequent abrasive polishing process. The surface is very flat and no obvious etching is observed, only shallow scratches induced by abrasives in the slurry can be observed. After removing a layer of material containing the overwhelming majority free carriers on the top surface by polishing, no etching occurs on the processed surface, which indicates that there are no excessive carriers exist on the processed surface. Although the mass difference is too small to be detected through weighing method, the thickness of material removal can be deduced from the MRR of CMP process. As mentioned above, the material removal rate is about 100 nm/h in the CMP process and the material removal is calculated to be around 1 μm after 9 h of

CMP. In conclusion, it can be concluded that the carriers are accumulated within 1 μm beneath the surface. Fig. 2(f) shows the surface morphology of sample V that only CMP was conducted on the surface. The scattered hexagonal-shaped etching pits on the surface indicate the lower density of excessive carriers. Although CMP has removed the high-density carrier accumulation layer just beneath the surface, there will always be scattered excessive carriers relatively far from the surface. Although applying an inverse electric field can extinguish the scattered excessive carrier relatively far from the surface. However, it is difficult to completely reduce the excessive carrier density from a high value to zero near the surface. That's why the scratches on the surface of sample III are slightly etched. The above results reveal the non-uniformity of carrier distribution along the vertical direction to the GaN surface. The density of carriers decreases from the outermost surface to the bulk material.

Based on the above results, it can be concluded that the carriers would be accumulated on the surface and change the surface energy after the electrochemical etching process. The change of surface energy will increase the chemical reaction activity and further cause severe surface oxidation during sample preservation.

To investigate the carrier accumulation's effect on surface oxidation, a comparison was made between an as-received sample and an electrochemically etched sample. As mentioned above, the carrier density is uniform throughout the bulk as-received sample, and relatively high on the surface of electrochemically etched sample. After both samples were kept in the atmosphere for over a month to ensure the full progress of the surface oxidation, the chemical composition and surface morphology and chemical composition of these two surfaces was examined by XPS and AFM, respectively. The sampling region of the electrochemically etched sample is outside the 8 mm electrochemical etching area. The initial surface is very smooth, and can be considered as the carrier-accumulated surface.

The core-level spectra of Ga3d for the as-received surface are shown in Fig. 3(a). The Ga 3d spectra can be fitted with four components: Ga—N (BE: 19.7 eV), Ga—O (BE: 20.6 eV), metal Ga (BE: 17.7 eV) and N2s (BE: 16.0 eV) [37–39]. The intensity ratio of Ga-O/Ga-N was estimated to compare the extent of surface oxidation. The Ga-O/Ga-N ratio of GaN surface was 0.158. The existence of Ga—O bonds could be

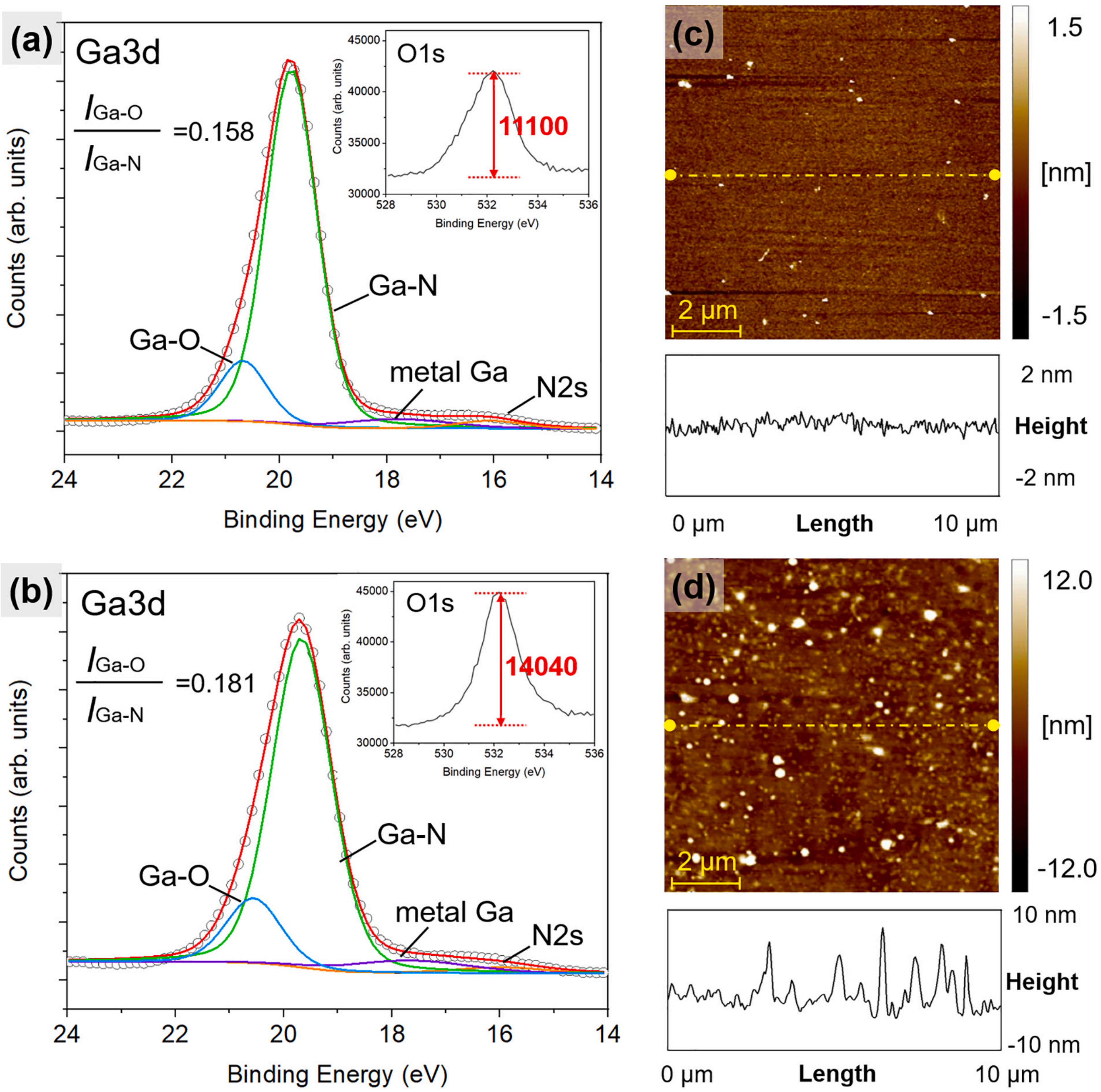

**Fig. 3.** (a, b) Core-level Ga3d XPS spectra and O1s spectra (inlet) of (a) as-received surface and (b) carrier-accumulated surface. (c, d) AFM images and surface profiles of the GaN surface of (c) an as-received sample kept in the atmosphere and (d) an electrochemically etched sample kept in the atmosphere.

attributed to the native oxide or the residual oxide formed by the precious CMP process. Fig. 3(b) shows the core-level spectra of Ga3d of the carrier-accumulated surface. There is no obvious change in the binding energies of above peaks. The Ga-O/Ga-N ratio of GaN surface was 0.181, which is larger than that of as-received surface. Meanwhile, the intensity of N2s peak deceases. The inlets in Fig. 3(a) and (b) also show the O1s spectra of two surfaces, respectively. The O1s intensity of the ae-received surface is higher than that of the carrier-accumulated surface. The above results indicate a more severe surface oxidation on the surface with accumulated carriers.

Fig. 3(c) shows the AFM image of the surface of the as-received surface kept in the atmosphere. This surface is comparatively smooth that only some surface contaminations can be observed rather than severe surface oxidation. For the as-received sample, the surface carrier density is small and evenly distributed. Hence, the surface is oxidized mildly by oxygen in the atmosphere and forms an oxide layer with a uniform thickness. Fig. 3(d) shows the AFM image of the carrier-accumulated surface kept in the atmosphere. Different from the as-received surface, many larger protrusions are generated on the surface which could be attributed to the severe surface oxidation with. The carriers accumulated on the surface would act as catalysts that provide surface energy in the oxidation process. Hence, the carrier-accumulated surface is more likely to be severely oxidized in the atmosphere. Due to the uneven distribution of carriers on the surface, the surface oxides generated on the surface also show high nonuniformity which will lead to high surface roughness and deteriorate the surface quality.

For an as-received GaN substrate without any treatment, the number of holes and electrons are in dynamic equilibrium since the rates of excitation and recombination are equal. The holes are minority carriers in the n-type GaN, which results in its low density on the surface. That is the reason why GaN cannot be etched just by immersing it in NaOH solution at room temperature. After applying an external electric field, there are two main modes of carrier movement in the GaN substrate. These two modes are the drift under the action of the external electric field and the diffusion due to the carrier density gradient [40]. The effect of the electric field on the movement of carriers is greater than that of spontaneous diffusion, resulting in the accumulation of excessive carriers on the surface.

The lifetime of excessive carriers is on the nanosecond scale as measured by time-resolved photoluminescence (TR PL) [41]. In theory, the excessive holes excited by the electric field will diffuse from the Ga-face to the N-face and recombine with the electrons in a very short duration. But in real situations, when the electric field is removed, the carrier distribution will not return to its original state even after a long period of time. A built-in electric field is formed and plays the role of attracting the carriers, which inhibits its spontaneous diffusion process caused by the density gradient. The formation of this built-in electric field may involve many factors, such as the surrounding atmosphere (especially oxygen) or the doping atoms. The actual formation principle of carrier accumulation still needs further investigation.

In conclusion, the accumulation of surface carriers has an adverse effect on the preservation of samples and should be prohibited. The effect of the relatively severe surface oxidation caused by carrier accumulation on the device performance needs further research. The etching process involving an electric field acting on the polar facets should be carefully considered. Applying an inverse electric field or removing the outermost material after electrochemical etching would be helpful for the release of the surface carrier accumulation effect.

### 3.2. Two etching modes tuned by carrier

In the previous section, we have revealed that the surface carrier density plays an important role in material removal during the electrochemical etching process. Also, tuning of the surface carrier density by applying an external electric field has been carried out. Additionally, we found that as the surface carrier density decreases, the etched surface morphology will change from protrusion to pit. In this section, the relationship between the carrier density and material removal mode in electrochemical etching process is discussed.

One sample was prepared by electrochemical etching and has a high surface carrier density, the other sample was prepared by electrochemical etching and subsequent inverse electric field to have a lower surface carrier density. The conditions of the electrochemical etching and application of the inverse electric field were the same as conditions in the previous section.

Fig. 4(a) shows the morphology of a scratched GaN surface with high carrier density etched in NaOH solution. After electrochemical etching, many protrusions are formed on the etched surface. It is worth noting that the scratches on the as-received surface will evolve into a row of closely arranged protrusions. In the previous studies, we have demonstrated that the products of electrochemical etching will dissolve in the electrolyte [36], which means that higher surface has less material removal. It can be concluded that the area where the protrusions are located has a lower etching rate in the electrochemical etching.

Since the width of the scratch induced by CMP process is only nanometers, it cannot be detected by PL due to its limited accuracy. Hence, a scratch with a width of about 10 μm was intentionally induced onto the surface using a diamond cutter as shown in Fig. 4(b). As shown in Fig. 4(c), the PL intensity along the scratch is relatively low compared to the as-received surface. The PL intensity is proportional to the number of photons emitting from the GaN substrate [42]. Hence, the decrease in PL intensity at the scratch indicates a decrease in the number of photons emitted there. When the surface is scratched by hard abrasives, it will leave subsurface damage beneath the scratches, which can be regarded as linear recombination center. The recombination center plays the role of inhibiting photons from escaping from the surface. During the electrochemical etching process, the recombination center will also lead to a reduction of local excessive carriers [26]. Therefore, only a few holes can get through the recombination centers and reach the GaN surface, so the etching rates along the scratches is low, and closely arranged protrusions will be formed on the surface.

Fig. 5(a) shows the AFM image of a scratched GaN surface with low carrier density etched in NaOH solution. Dense hexagonal-shaped etching pits are formed along the scratches, indicating that the material is mainly removed by a chemical etching process. Fig. 5(b) shows the morphology and cross-sectional profile of an etching pit from the surface shown in Fig. 5(a). From the cross-sectional profile, it is revealed that the depth of the etching pit is around 40 nm which is shallow compared to its 3 μm radial length. A platform is formed in the bottom of the etching pit which indicates the etching along the vertical direction is uniform.

The two samples are only affected by the electric field and only react with NaOH solution, so the chemical reactions occurring on them are the same. The charge carriers in the valence band obtain energy from the electric field and leaps into the conduction band and move to the outermost surface of GaN under the action of electric field. The carriers on the surface are consumed by hydroxyl ions and form an oxide layer. After that, the oxide layer is dissolved in the NaOH solution. The different etching characteristics are due to the two modes of material removal in etching, which depend on the surface excessive carrier density. Fig. 6 compares the formation mechanism of etched surface morphology under different carrier densities. Under low surface carrier density, the etching process is mainly determined by the etchants. The surface carriers can be considered as a sense of catalyst which reduces the activation energy required for chemical reactions, thus GaN can be etched by hydroxyl ions. The hydroxyl ions in the NaOH solution are absorbed on Ga dangling bonds somewhere with a relatively high density of carriers, breaking the Ga—N bonds and thus the etching begins [43]. The highly reactive region such as dislocations and scratches with Ga dangling bonds is preferential to be etched. The formation mechanism of hexagonal-shaped etching pits has been studied in detail [22,23]. The planar density is considered as the main factor that

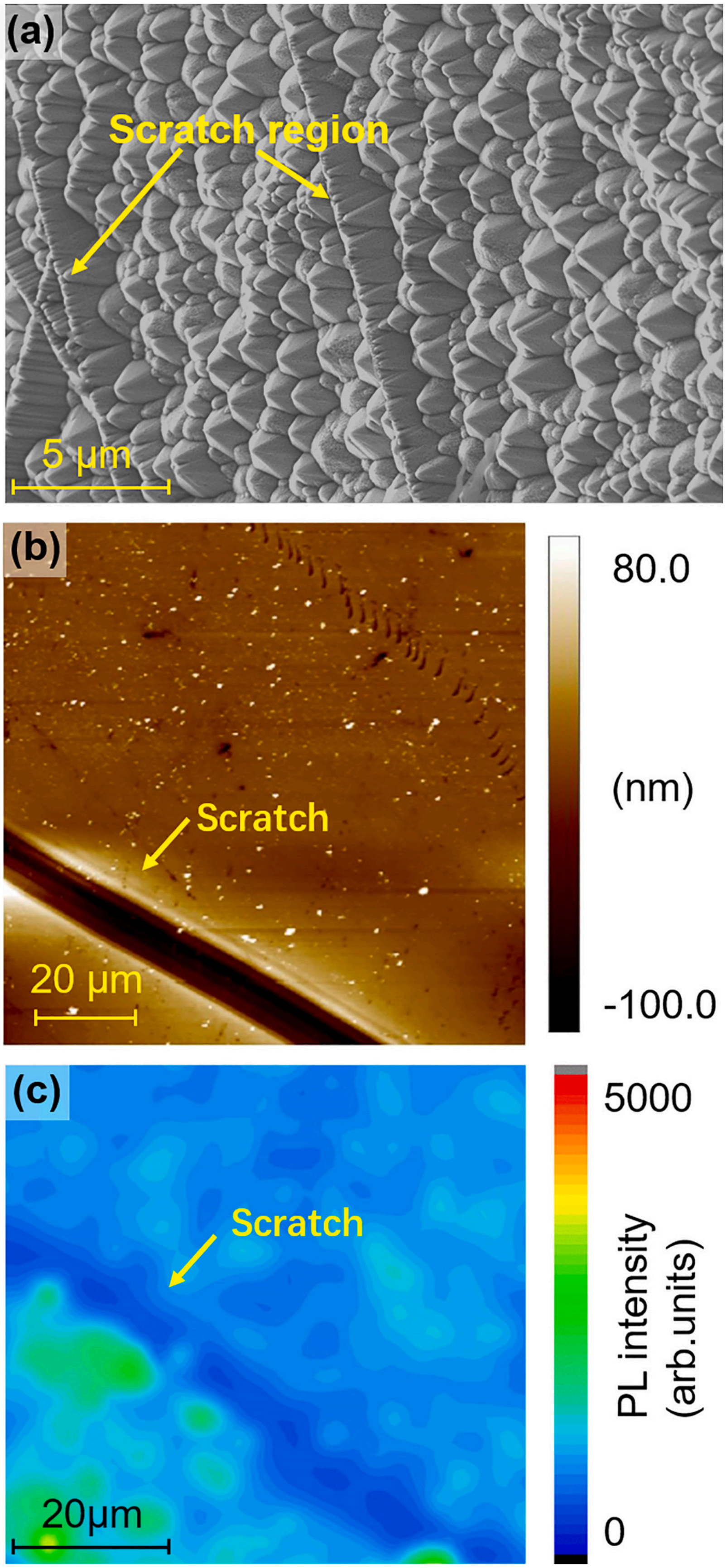

**Fig. 4.** (a) SEM image of a scratched GaN surface after electrochemical etching (The intersection angle of the electron beam and the surface was set to 45°); (b) AFM image of the GaN surface with an intentionally induced scratch using diamond cutter (c) PL intensity mapping of the GaN surface with an intentionally induced scratch using diamond cutter.

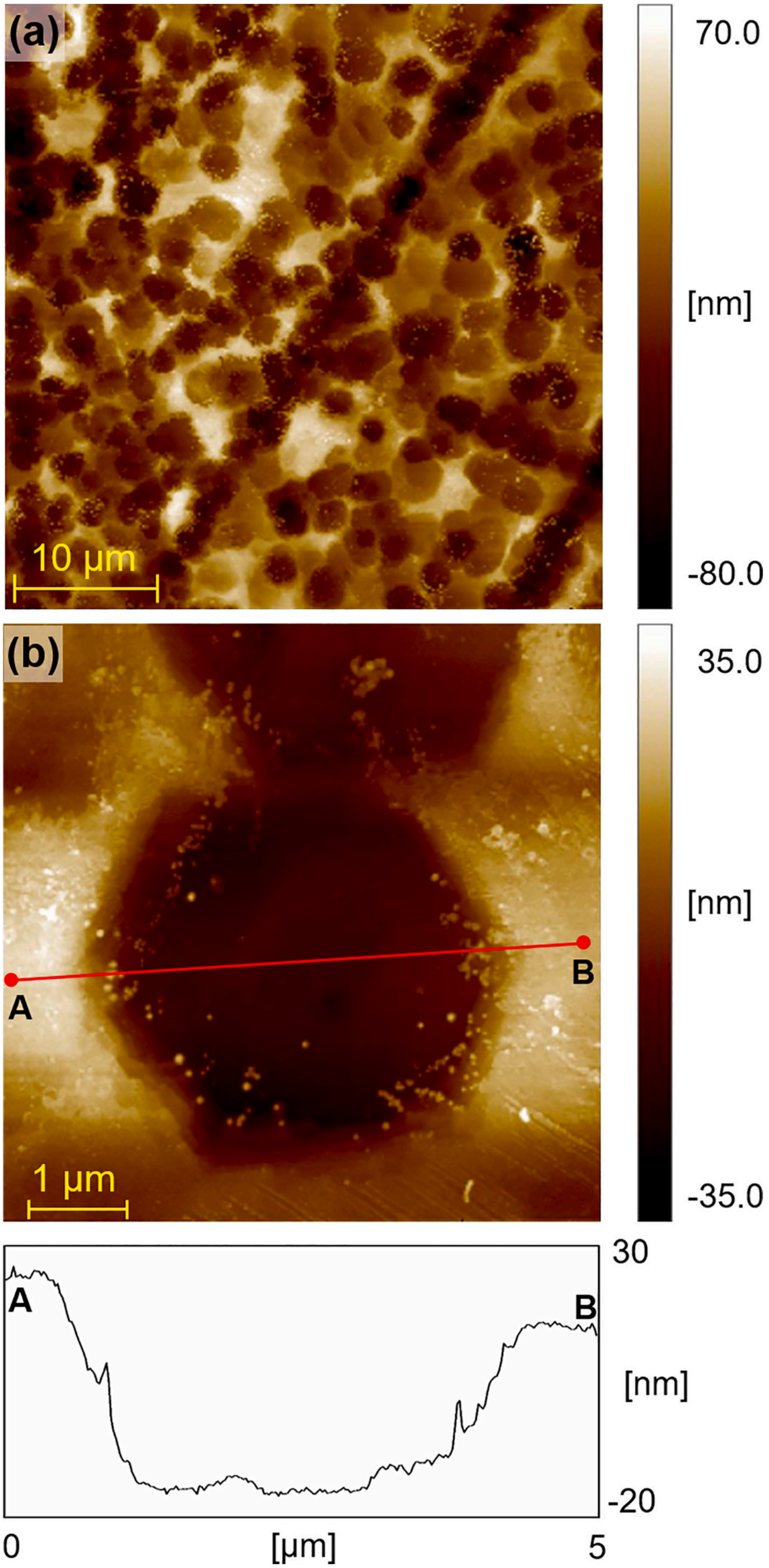

**Fig. 5.** (a) AFM images of GaN surface with a low excessive carrier density etched in the NaOH solution; (b) magnified AFM image and cross-sectional profile of an etching pit from (a).

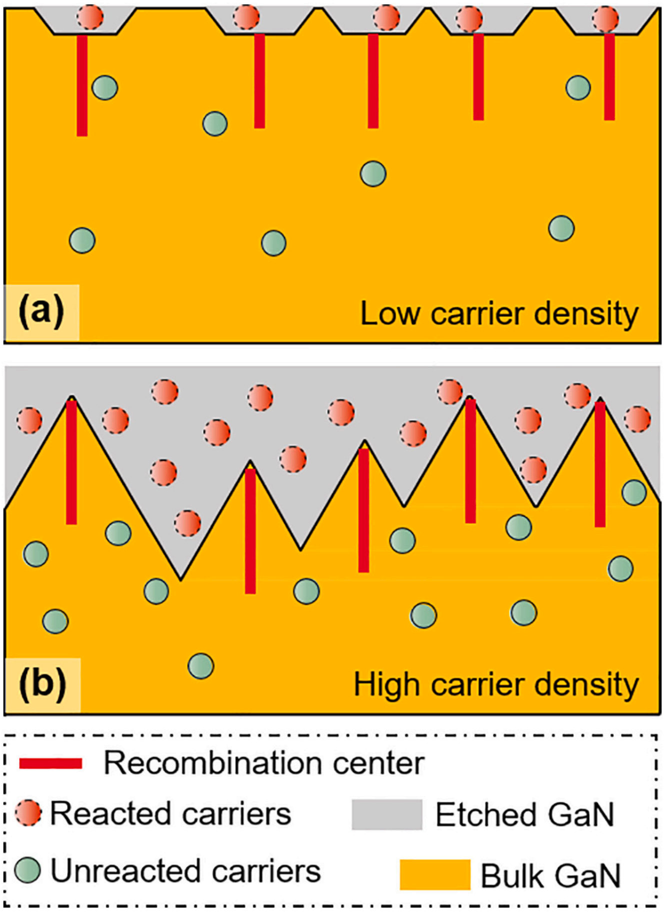

**Fig. 6.** The formation mechanism of surface morphology in the electrochemical etching: (a) under low carrier density; (b) under high carrier density. The red ball represents the carriers that have been reacted with NaOH solution. The green ball represents the carriers in the substrate that have not been reacted. The red line represents the recombination center. (For interpretation of the references to color in this figure legend, the reader is referred to the web version of this article.)

influences the etching rate. The planar density of the c-plane is larger than that of other facets, which results in the lowest etching rate of the c-plane. Hence, the material removal along the vertical direction is minimum. The planar density of the r-plane is smaller than other facets, which leads to a relatively high etching rate of the r-plane [43]. This makes the etching pits mainly expand along the direction perpendicular to the r-plane. The intersection angle between the r-plane and the surface is about 45°, thus forming the shallow and hexagonal-shaped etching pits.

Under high surface carrier density, the etching process is mainly affected by the surface excessive carrier. Abundant carriers are forced to the outermost surface under the action of external electric field. Although the chemistry is identical, the recombination center inhibits the carriers from drifting to the GaN surface and contacting with the OH- ions. The dislocations can also be considered as recombination centers. Therefore, the region where dislocation exists has a relatively low etching rate. As the distance between the carrier and the recombination center increases, the trap ability of the recombination center to the carrier decreases. Thus, the height of the region where dislocations exist becomes larger than that of other areas and form a morphology with many hexagonal-shaped protrusions. In the initial stage of etching under high carrier density, the etching also starts from a highly reactive point and expands into etching pits. For a perfect crystalline GaN substrate without recombination centers, the etched surface will be covered with the united or overlapped hexagonal-shaped etching pits.

### 3.3. Abrasion behavior after electrochemical etching treatment

In the above sections, the material removal mechanisms in electrochemical etching have been discussed from the perspective of carrier behavior. As previously stated, the surface carrier accumulation layer will deteriorate the surface quality. Besides, the surface is rough after the electrochemical etching owing to the formation of protrusions. Hence, the etched surface should be further processed by abrasion for achieve a smooth surface. In this section, the material removal mechanism in the subsequent abrasion process is discussed. The as-received surface was lapped to be rough using a diamond lapping pad with a grain size of about 15 μm (1000 #). After the electrochemical etching process, the entire GaN surface was mechanically polished using a diamond polishing pad with a grain size of about 5 μm (2500 #). In the lapping and mechanical polishing, the rotation speed of the polishing head and polishing pad were both 50 rpm, with an applied pressure of 0.5 kg/cm$^2$.

Fig. 7(a) shows the surface morphology of the interface between the non-etched area and the pre-etched area after mechanical polishing using abrasives with grain size of 5 μm. The surface morphologies exhibit a large discrepancy that many cracks and pits are formed on the non-etched surface, while the pre-etched surface is rather flat and only scratches can be observed. The AFM images of the non-etched area and pre-etched area after mechanical polishing are also shown in Fig. 7(b) and (c). As shown in Fig. 7(b), the non-etched GaN was fractured into large pieces due to its high brittleness, forming cracks and pits on the surface. The surface roughness of the non-etched surface after mechanical polishing was measured to be Sa28.5 nm. However, only scratches can be observed on the pre-etched surface as shown in Fig. 7 (c). The surface roughness of the pre-etched surface was measured to be Sa2.56 nm.

To investigate the hardness of the non-etched and pre-etched surface, nanoindentation tests were carried out after mechanical polishing. In the nanoindentation test, 12 points arranged in an array of 3 rows and 4 columns on the non-etched and pre-etched surface are tested, respectively. The spacing between each point is 10 μm, and the maximum indentation load was set to 1.0 mN. Fig. 7(d) shows the hardness values and nano-indentation curves of non-etched and pre-etched GaN surface after mechanical polishing. The nanoindentation curves show that the displacement of the indenter for the pre-etched and non-etched surface was only 62 nm and 52 nm, respectively. The hardness values are calculated from the nanoindentation curves by the Oliver-Pharr method [44]. The results show that the surface hardness of the non-etched surface is about 15.4 GPa, while the hardness of the pre-etched surface is only 10.9 GPa.

The surface chemical composition of the non-etched and pre-etched areas is the same as confirmed by XPS [36], thus, the decrease in surface hardness may be attributed to the change in surface structure. Fig. 7(e) shows the magnified SEM image of the pre-etched surface after mechanical polishing. Many nanoscale pores can be observed on the pre-etched area. These nanopores are supposed to be the reason for the improvement of ductility of the pre-etched region. We cut off the sample and tilt the sample stage to about 45° to observe the surface and cross-section of the sample simultaneously. A nano-channel layer with a thickness of about 500 nm is formed beneath the GaN surface, as shown in Fig. 7(f). The nano-channel layer can be considered as the extension of nanopores into the bulk material. The formation of the nano-channel layer can be attributed to the breakdown on account of electric field concentration on the protrusions [36]. From the results of nano-indentation test, it can be concluded that the nano-channel layer has a smaller hardness and better ductility than that of the original GaN. Therefore, the nano-channel layer is easier to be removed during the abrasive machining process. In summary, the increased ductility of nano-channel layer would make abrasives induce less damage and

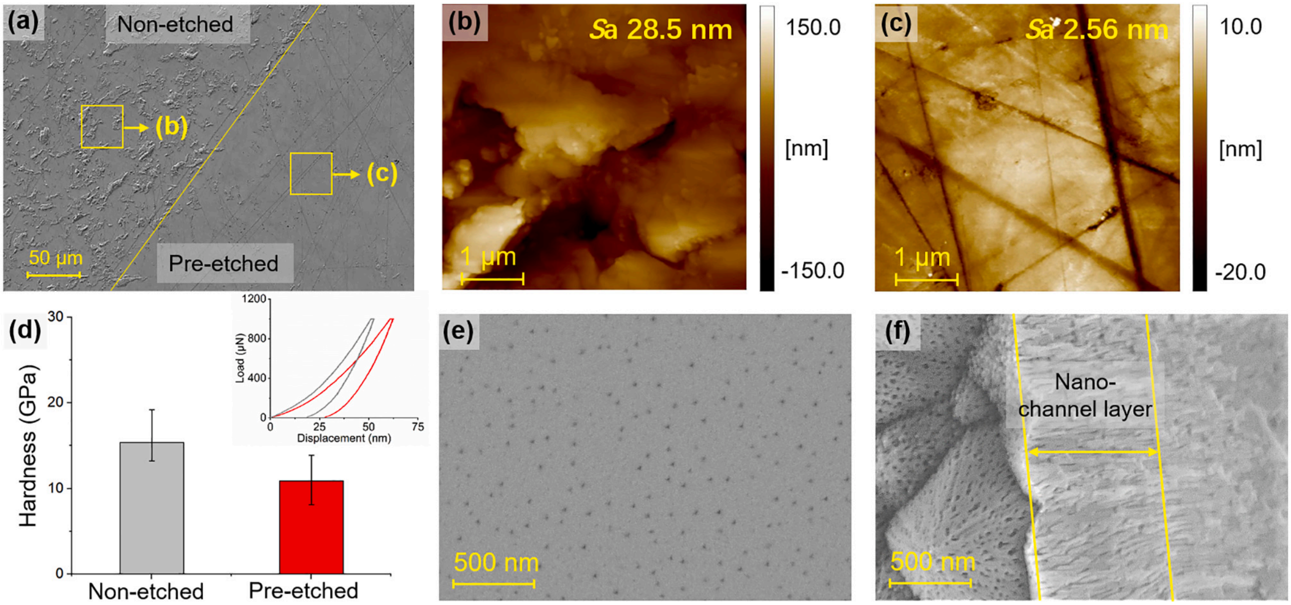

**Fig. 7.** (a) Surface morphology of the interface between the non-etched area and the pre-etched area after mechanical polishing using abrasives with grain size of 5 μm. (b, c) AFM images of the (b) non-etched surface (Sa: 28.5 nm) and (c) pre-etched surface (Sa: 2.56 nm) after mechanical polishing using abrasives with grain size of 5 μm. (d) load-displacement curves and hardness calculated from the measured data for the non-etched surface and pre-etched surface. (e) Nanopores left on the surface after mechanical polishing. (f) nano-channel layer formed in the electrochemical etching.

achieve better surface roughness.

Two-dimensional PL mapping measurement was conducted to evaluate the surface quality of the pre-etched and non-etched GaN surface after the polishing process [45]. The data was collected from an area with a dimension of 100 μm × 100 μm. A total of 225 sampling points were examined, with 15 points on the x-axis and 15 points on the y-axis.

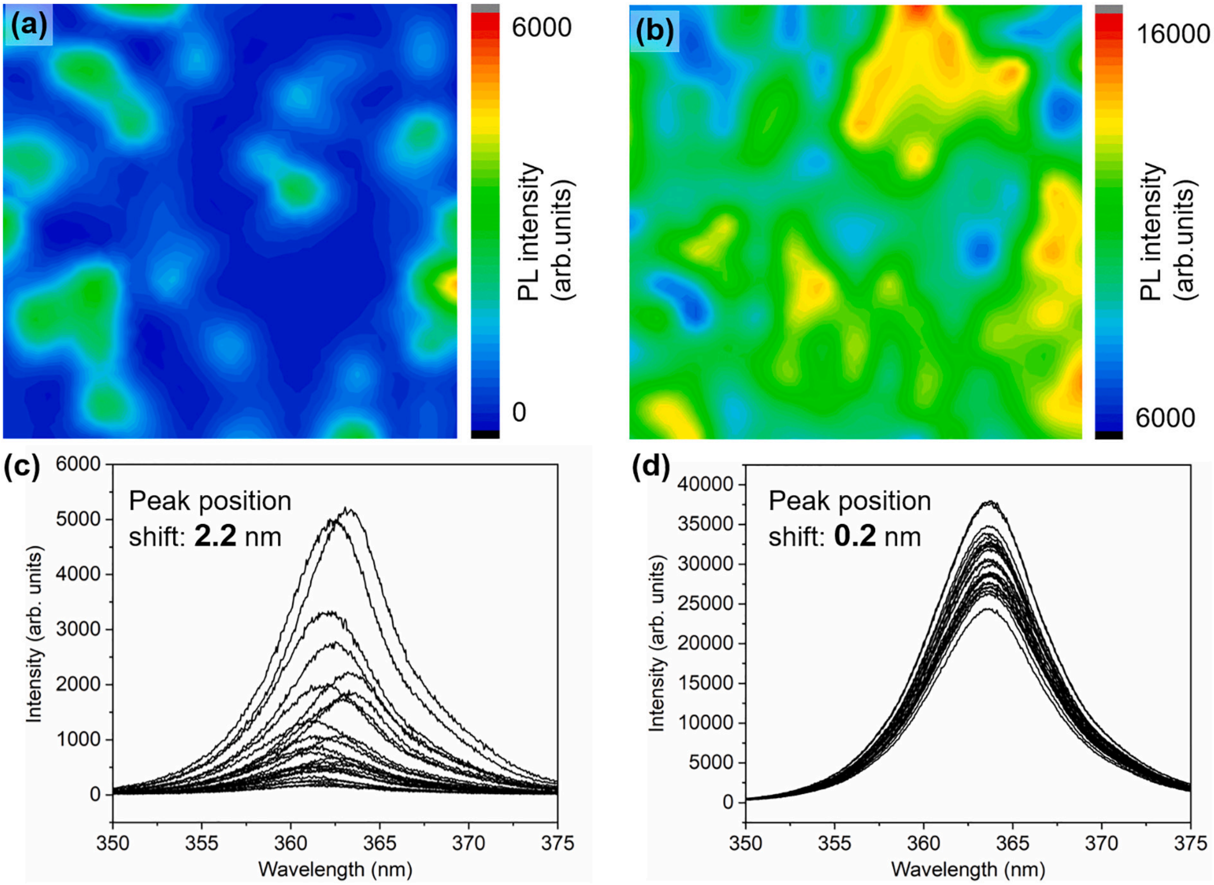

**Fig. 8.** PL intensities of a mechanically polished GaN: (a) non-etched surface and (b) pre-etched surface, (c, d) 25 sets of PL spectra selected from (a) and (b), respectively.

The distance between each point is about 6.67 μm. Fig. 8(a) shows the PL intensities of the non-etched surface after mechanical polishing. The values of PL intensity are collected in the wavelength range of from 350 nm to 375 nm and take the average. The PL intensities of many locations on the non-etched surface are close to zero, indicating the existence of subsurface damage. The formation of subsurface damage is the result of brittle removal using abrasives with large grain size in mechanical polishing. Fig. 8(b) shows the PL intensities of the pre-etched surface after mechanical polishing. As a whole, the pre-etched surface exhibits a much higher PL intensity compared to the non-etched surface. This might be due to the high surface area of the porous structure which emits more photons under the excitation of the ultraviolet laser [40,42]. It is worth noting that the ratio of the maximum value to the minimum value is only about twice of magnitude for the pre-etched surface, while is about two orders for the non-etched surface. Besides, the PL intensities at any point on the surface are not close to zero and better uniformity has been demonstrated, which also indicates the desirable surface integrity of the pre-etched area after mechanical polishing. The slight inhomogeneity of PL intensity could be attributed to the uneven distribution of surface carriers.

We also compare the peak positions of the above two regions. 25 sets of data that are sufficient to distinguish the difference between the two regions were randomly selected. Fig. 8(c) shows that the PL peak positions of the non-etched region lack consistency and have a wide range from 361.1 nm to 363.3 nm. All PL peak positions show varying degrees of red-shift due to the residual stress induced by mechanical polishing [46,47]. However, as shown in Fig. 8(d), the PL peak positions of the pre-etched surface have a very small shifting range of 0.2 nm, and they are all close to 363.8 nm. The good consistency of pre-etched surface PL spectra indicates the higher surface integrity.

In conclusion, the nanochannel layer can be considered as a modified layer resulting from electrochemical etching. This layer has good ductility that the material is not removed in a brittle mode in abrasion. After mechanical polishing, this residual nanochannel layer shows a good surface quality and a relatively low surface roughness. The surface planarization by mechanical polishing is relatively more efficient, and the residual nanochannel layer can be removed by the final CMP process in a short duration. Therefore, the electrochemical etching combined with mechanical polishing can be considered as a semi-finishing technique. In this process, the electrochemical etching would efficiently remove the damaged layer induced by grinding or lapping, and the subsequent mechanical polishing would rapidly reduce the surface roughness and remove most of the nanochannel layer.

## 4. Conclusion

To reveal the material removal mechanisms in electrochemical etching-enhanced polishing of GaN, a series of experiments have been conducted and the following conclusions can be drawn from this study:

1. The electric field could alter the distribution of excessive carriers along the polar plane of GaN. After the electrochemical etching, the excessive carriers are accumulated on the surface and would not return to their original state spontaneously. The accumulation of excessive carriers has an adverse effect on sample preservation and should be prohibited.
2. The dislocations and subsurface damage act as recombination centers and trap the free excessive carriers, resulting in a local low etching rate. Under higher carrier density, the carriers are abundant so the surface morphology is determined by the locations of recombination centers. Under low carrier density, the material removal is achieved through a chemical etching process. The surface morphology is mainly determined by the locations of highly reactive dangling bonds on the surface.
3. A nano-channel layer would be formed along the vertical direction of the GaN surface through electrochemical etching. The surface hardness of the pre-etched surface with nano-channel layer is relatively low compared to the non-etched GaN surface which is easier to be removed in the following mechanical polishing process. Electrochemical etching combined with mechanical polishing can be considered as a semi-final processing technique with high removal rate and relatively good surface integrity.

## Declaration of competing interest

The authors declare that they have no known competing financial interests or personal relationships that could have appeared to influence the work reported in this paper.

## Acknowledgements

This work is financially supported by the National Natural Science Foundation of China (Grant No. 52035009, 52005243) and the research fund from the Science, Technology and Innovation Commission of Shenzhen Municipality (JCYJ20200109141003910), Shenzhen, China. The authors acknowledge the assistance of SUSTech Core Research Facilities.

## References

[1] Fletcher ASA, Nirmal D. A survey of gallium nitride HEMT for RF and high power applications. Superlattice Microst 2017;109:519–37.

[2] Shinohara K. Chapter four - III-nitride millimeter wave transistors. In: Chu R, Shinohara K, editors. Semiconductors and semimetals. Elsevier; 2019. p. 141–84.

[3] Chander S, Gupta S, Ajay Gupta M. Enhancement of breakdown voltage in AlGaN/GaN HEMT using passivation technique for microwave application. Superlattice Microst 2018;120:217–22.

[4] Takimoto T, Takeshita K, Nakamura S, Okumura T. Effects of plasma-induced defects on electrical characteristics of AlGaN/GaN heterostructure before and after low-temperature annealing. Thin Solid Films 2014;557:212–5.

[5] Bhat I. 3 - physical properties of gallium nitride and related III–V nitrides. In: Baliga BJ, editor. Wide bandgap semiconductor power devices. Woodhead Publishing; 2019. p. 43–77.

[6] Qin H, Luan X, Feng C, Yang D, Zhang G. Mechanical, thermodynamic and electronic properties of wurtzite and zinc-blende GaN crystals. Materials 2017;10(12):1419.

[7] Aida H, Doi T, Takeda H, Katakura H, Kim S-W, Koyama K, Yamazaki T, Uneda M. Ultraprecision CMP for sapphire, GaN, and SiC for advanced optoelectronics materials. Curr Appl Phys 2012;12:S41-S46.

[8] Aida H, Kim S-W, Ikejiri K, Doi T, Yamazaki T, Seshimo K, Koyama K, Takeda H, Aota N. Precise mechanical polishing of brittle materials with free diamond abrasives dispersed in micro–nano-bubble water. Precis Eng 2015;40:81–6.

[9] Aida H, Takeda H, Kim S-W, Aota N, Koyama K, Yamazaki T, Doi T. Evaluation of subsurface damage in GaN substrate induced by mechanical polishing with diamond abrasives. Appl Surf Sci 2014;292:531–6.

[10] Aida H. 8 - Chemical and physical mechanisms of CMP of gallium nitride. In: Babu S, editor. Advances in chemical mechanical planarization (CMP). Woodhead Publishing; 2016. p. 187–212.

[11] Jiang Q, Zhang L, Yang C. Research on material removal mechanism and radial cracks during scribing single crystal gallium nitride. Ceram Int 2021;47(11):15155–64.

[12] Aida H, Takeda H, Koyama K, Katakura H, Sunakawa K, Doi T. Chemical mechanical polishing of gallium nitride with colloidal silica. J Electrochem Soc 2011;158(12). H1206-H1212.

[13] Aida H, Takeda H, Aota N, Kim SW, Koyama K. Surface treatment for GaN substrate -comparison of chemical mechanical polishing and inductively coupled plasma dry etching. Sens Mater 2013;25(3):189–204.

[14] Baik KH, Pearton SJ. Dry etching characteristics of GaN for blue/green light-emitting diode fabrication. Appl Surf Sci 2009;255(11):5948–51.

[15] Zhou S, Cao B, Liu S. Dry etching characteristics of GaN using Cl2/BCl3 inductively coupled plasmas. Appl Surf Sci 2010;257(3):905–10.

[16] Terano A, Imadate H, Shiojima K. Mapping etching induced damages on GaN surfaces using scanning internal photoemission microscopy. Mater Sci Semicond Process 2017;70:92–8.

[17] Ismail MR, Basirun WJ. Chemical wet etching of silicon wafers from a mixture of concentrated acids. Adv Mat Res 2011;264–265:1027–32.

[18] Zhuang D, Edgar JH. Wet etching of GaN, AlN, and SiC: a review. Mater Sci Eng R Rep 2005;48(1):1–46.

[19] Vartuli CB, Pearton SJ, Abernathy CR, MacKenzie JD, Ren F, Zolper JC, Shul RJ. Wet chemical etching survey of III-nitrides. Solid State Electron 1997;41(12):1947–51.

[20] Hong SK, Kim BJ, Park HS, Park Y, Kim TI. Evaluation of nanopipes in MOCVD grown (0001) GaN/Al2O3 by wet chemical etching. J Cryst Growth 1998;191(1–2):275–8.

[21] Shiojima K. Atomic force microscopy and transmission electron microscopy observations of KOH-etched GaN surfaces. J Vac Sci Technol, B: Microelectron Nanometer Struct–Process, Meas, Phenom 2000;18(1):37.

[22] Kozawa T, Kachi T, Ohwaki T, Taga Y, Koide N, Koike M. Dislocation etch pits in GaN epitaxial layers grown on sapphire substrates. J Electrochem Soc 1996;143(1):L17–9.

[23] Zhang L, Shao Y, Wu Y, Hao X, Chen X, Qu S, Xu X. Characterization of dislocation etch pits in HVPE-grown GaN using different wet chemical etching methods. J Alloys Compd 2010;504(1):186–91.

[24] Hong SK, Yao T, Kim BJ, Yoon SY, Kim TI. Origin of hexagonal-shaped etch pits formed in (0001) GaN films. Appl Phys Lett 2000;77(1):82–4.

[25] Palacios T, Calle F, Varela M, Ballesteros C, Muoz E. Wet etching of GaN grown by molecular beam epitaxy on Si(111). Semicond Sci Technol 2000;15(10):996.

[26] Murata J, Sadakuni S. Photo-electrochemical etching of free-standing GaN wafer surfaces grown by hydride vapor phase epitaxy. Electrochim Acta 2015;171:89–95.

[27] Weyher JL, Smalc-Koziorowska J, Bańkowska M, Dzięcielewski I, Marona Ł, Perlin P. Photo-etching of GaN: revealing nano-scale non-homogeneities. J Cryst Growth 2015;426:153–8.

[28] Matsumoto S, Toguchi M, Takeda K, Narita T, Kachi T, Sato T. Effects of a photo-assisted electrochemical etching process removing dry-etching damage in GaN. Jpn J Appl Phys 2018;57(12):121001.

[29] Yang X, Yang X, Sun R, Kawai K, Arima K, Yamamura K. Obtaining atomically smooth 4H–SiC (0001) surface by controlling balance between anodizing and polishing in electrochemical mechanical polishing. Nanomanuf Metrol 2019;2(3):140–7.

[30] Visconti P, Jones KM, Reshchikov MA, Cingolani R, Morkoç H, Molnar RJ, Smith DJ. Defect investigation of GaN thin films etched by photo-electrochemical and hot wet etching by atomic force and transmission electron microscopy. MRS Proc 2011;680(E5):8.

[31] Griffin PH, Oliver RA. Porous nitride semiconductors reviewed. J Phys D Appl Phys 2020;53(38):383002.

[32] Ou L, Dong Z, Kang R, Shi K, Guo D. Photoelectrochemically combined mechanical polishing of n-type gallium nitride wafer by using metal nanoparticles as photocathodes. Int J Adv Manuf Technol 2019;105(11):4483–9.

[33] Dong Z, Ou L, Kang R, Hu H, Zhang B, Guo D, Shi K. Photoelectrochemical mechanical polishing method for n-type gallium nitride. CIRP Ann 2019;68(1):205–8.

[34] Cao D, Xiao H, Mao H, Ma H, Gao Q, Liu J, Ma J, Liu X. Electrochemical characteristics of n-type GaN in oxalic acid solution under the pre-breakdown condition. J Alloys Compd 2015;652:200–4.

[35] Nowak G, Xia XH, Kelly JJ. Electrochemical etching of highly conductive GaN single crystals. J Cryst Growth 2001;222(4):735–40.

[36] Zhang L, Deng H. Highly efficient and damage-free polishing of GaN (0001) by electrochemical etching-enhanced CMP process. Appl Surf Sci 2020;514:145957.

[37] Hsu HC, Su YK, Cheng SH, Huang SJ, Ca OJM, Chen KC. Investigation of etch characteristics of non-polar GaN by wet chemical etching. Appl Surf Sci 2010;257(3):1080–3.

[38] Grodzicki M, Mazur P, Zuber S, Brona J, Ciszewski A. Oxidation of GaN(0001) by low-energy ion bombardment. Appl Surf Sci 2014;304:20–3.

[39] Huang R, Liu T, Zhao Y, Zhu Y, Huang Z, Li F, Liu J, Zhang L, Zhang S, Dingsun A, Yang H. Angular dependent XPS study of surface band bending on ga-polar n-GaN. Appl Surf Sci 2018;440:637–42.

[40] Al-Heuseen K, Hashim MR, Ali NK. Effect of different electrolytes on porous GaN using photo-electrochemical etching. Appl Surf Sci 2011;257(14):6197–201.

[41] Watanabe H, Kato M, Ichimura M, Arai E, Kanechika M, Ishiguro O, Kachi T. Excess carrier lifetime measurement for plasma-etched GaN by the microwave photoconductivity decay method. Jpn J Appl Phys 2007;46(1):35–9.

[42] Al-Heuseen K, Hashim MR. Enhancing hydrogen sensitivity of porous GaN by using simple and low cost photoelectrochemical etching techniques. Sensors Actuators B Chem 2012;163(1):159–64.

[43] Lai Y-Y, Hsu S-C, Chang H-S, Wu YS, Chen C-H, Chen L-Y, Cheng Y-J. The study of wet etching on GaN surface by potassium hydroxide solution. Res Chem Intermed 2016;43(6):3563–72.

[44] Oliver WC, Pharr GM. An improved technique for determining hardness and elastic modulus using load and displacement sensing indentation experiments. J Mater Res 2011;7(6):1564–83.

[45] Song Y, Xu Z, Li R, Wang H, Fan Y, Rommel M, Liu J, Astakhov GV, Hlawacek G, Li B, Xu J, Fang F. Photoluminescence and raman spectroscopy study on color centers of helium ion-implanted 4H–SiC. Nanomanuf Metrol 2020;3(3):205–17.

[46] Cheah SF, Lee SC, Ng SS, Yam FK, Abu Hassan H, Hassan Z. Luminescence evolution of porous GaN thin films prepared via UV-assisted electrochemical etching. JOL 2015;159:303–11.

[47] Yam FK, Hassan Z, Ng SS. Porous GaN prepared by UV assisted electrochemical etching. Thin Solid Films 2007;515(7–8):3469–74.